Observation of the spin Seebeck effect in epitaxial Fe_3O_4 thin films

R. Ramos,[1,a)] T. Kikkawa,[2] K. Uchida,[2,3] H. Adachi,[4,5] I. Lucas,[6] M. H. Aguirre,[1] P. Algarabel,[6] L. Morellón,[1,7] S. Maekawa,[4,5] E. Saitoh,[2,4,5,8] and M. R. Ibarra[1,7]
[1]*Instituto de Nanociencia de Aragón, Universidad de Zaragoza, E-50018 Zaragoza, Spain*
[2]*Institute for Materials Research, Tohoku University, Sendai 980-8577, Japan*
[3]*PRESTO, Japan Science and Technology Agency, Kawaguchi, Saitama 332-0012, Japan*
[4]*Advanced Science Research Center, Japan Atomic Energy Agency, Tokai 319-1195, Japan*
[5]*CREST, Japan Science and Technology Agency, Sanbancho, Tokyo 102-0075, Japan*
[6]*Instituto de Ciencia de Materiales de Aragón, Universidad de Zaragoza and Consejo Superior de Investigaciones Científicas, 50009 Zaragoza, Spain*
[7]*Departamento de Física de la Materia Condensada, Universidad de Zaragoza, E-50009 Zaragoza, Spain*
[8]*WPI Advanced Institute for Materials Research, Tohoku University, Sendai 980-8577, Japan*

(Received 13 December 2012; accepted 12 February 2013; published online 22 February 2013)

We report the experimental observation of the spin Seebeck effect in magnetite thin films. The signal observed at temperatures above the Verwey transition is a contribution from both the anomalous Nernst (ANE) and spin Seebeck (SSE) effects. The contribution from the ANE of the Fe_3O_4 layer to the SSE is found to be negligible due to the resistivity difference between Fe_3O_4 and Pt layers. Below the Verwey transition, the SSE is free from the ANE of the ferromagnetic layer and it is also found to dominate over the ANE due to magnetic proximity effect on the Pt layer. © *2013 American Institute of Physics*. [http://dx.doi.org/10.1063/1.4793486]

Thermoelectric effects result from the combination between charge and heat current in suitable materials having applications as electric cooling systems or thermal power generators. Despite decades of research into thermoelectric materials and properties, the efficiency of thermoelectric devices has remained low due to the interdependence of the Seebeck voltage, S, the resistivity, ρ, and the thermal conductivity, κ.[1,2] One promising approach to overcome this problem and increase the versatility of thermoelectric devices involves exploiting the spin of the electron, in addition to its charge and heat transport properties. This is the main interest of spin caloritronics.[3–9] Since the discovery of the spin Seebeck effect (SSE),[10] this field has been the focus of intensive theoretical and experimental research, with the recent detection among others of the spin-dependent Seebeck[11] and Peltier effects.[12] The SSE consists in the generation of a spin voltage in a ferromagnet as a result of an applied thermal gradient in magnetic materials, and this spin voltage can be detected with an adjacent paramagnetic metal by means of the inverse spin Hall effect (ISHE).[13] Since its discovery in permalloy,[10] the SSE has been measured in spin polarized metals,[14] semiconductors,[15–17] and insulators.[18] In contrast to conventional thermoelectrics, this effect offers the possibility for another approach in all-solid state energy conversion devices, since it involves properties of at least two different materials that can be optimized independently. One example is the recent enhancement of the spin Seebeck effect by implementation of a spin Hall thermopile structure.[19]

The SSE is explained in terms of a spin current injected from the ferromagnet (FM) into the paramagnetic metal (PM), which is scattered by the ISHE, generating an electric field $\vec{E}_{ISHE}$ given by

$$\vec{E}_{ISHE} = \frac{\theta_{SH}\rho}{A}\left(\frac{2e}{\hbar}\right)\vec{J}_S \times \vec{\sigma}, \tag{1}$$

where θ_{SH}, ρ, A, e, $\vec{J}_S$, and $\vec{\sigma}$ are the spin-Hall angle of PM, electric resistivity of PM, contact area between FM and PM, electron charge, spin current across the FM/PM interface, and the spin polarization of FM, respectively. The spin current $\vec{J}_S$ is generated as the result of a thermal non-equilibrium between magnons in FM and a conduction-electron spin accumulation in PM, which interact through the s-d exchange coupling J_{sd} at the FM/PM interface. Using the linear-response approach, the spin current injected into PM is calculated to be[20,21]

$$J_s = -G_S k_B\left(T^*_{FM} - T^*_{PM}\right), \tag{2}$$

where T^*_{FM} and T^*_{PM} are the effective magnon temperature in FM and the effective conduction-electron temperature in PM, and $G_S = \frac{J^2_{sd} S_0 \chi_N \tau_{sf}}{\hbar}$ with S_0, χ_N, and τ_{sf} being, respectively, the size of the localized spin in FM, the paramagnetic susceptibility, and spin flip relaxation time in PM. A similar interpretation has been developed using the scattering approach.[22]

In this letter, we report the experimental observation of the spin Seebeck effect in magnetite. Magnetite is a ferrimagnetic oxide with a predicted half metallic character and a high Curie temperature (858 K), and these properties have inspired investigations for possible spintronic applications;[23] therefore, films and heterostructures of this material have been grown by several techniques.[24–27] Besides, magnetite possesses a metal-insulator transition at around 121 K, known as the Verwey transition.[28]

A Fe_3O_4 (001) film (FM) of thickness $t_I = 50$ nm was deposited on a $SrTiO_3$ (001) substrate of thickness $t_{STO} = 0.5$ mm, by pulsed laser deposition (PLD) using a KrF

a)ramosr@unizar.es.

 © 2013 American Institute of Physics

This article is copyrighted as indicated in the article. Reuse of AIP content is subject to the terms at: http://scitation.aip.org/termsconditions. Downloaded to IP: 161.111.180.191 On: Wed, 08 Jul 2015 09:55:11

excimer laser with 248 nm wavelength, 10 Hz repetition rate, and 3×10^9 W/cm^2 irradiance in an ultrahigh-vacuum chamber. The film thickness was measured by x-ray reflectivity (XRR). The Verwey transition temperature of the film was measured with SQUID magnetometer and four probe resistivity measurements and has a value of $T_V = 115$ K and the room temperature resistivity is 5 mΩ cm. Further details on the growth and characterization can be found elsewhere.[29]

The SSE was measured using the so called longitudinal configuration[30] (see Fig. 1(a)); a temperature gradient (∇T) is applied in the $\mp z$ direction, generating a temperature difference ($\pm \Delta T$) between the bottom and the top of the sample, with temperatures $T \pm \Delta T$ and T, respectively. The voltage (V_y) is measured along the y direction, while a sweeping magnetic field is applied at an angle θ with respect to the x direction. This configuration is normally used for insulating samples, for measurements performed on electrically conductive samples with this geometry; the anomalous Nernst effect (ANE)[31] is also measured along with the SSE. In order to separate the contribution of the ANE, simultaneous measurements of both effects were performed on the same Fe_3O_4 film; to do this, two equal pieces with a length of $L_y = 8$ mm and a width of $L_x = 4$ mm were cut and a Pt layer (PM) of thickness $t_{II} = 5$ nm was deposited on one of them, and both samples were loaded at the same time and kept under the same experimental conditions.

Figure 1(b) shows the results obtained at 300 K on the magnetic field dependence of the transversal voltage (V_y), measured on samples with and without the Pt layer. It is interesting to observe a strong enhancement of the signal upon placement of the spin detection layer (5 nm Pt), which is increased by ~4 times with respect to that observed with no Pt layer. The fact that the resistivity at room temperature of the magnetite layer is 5 mΩ cm which is about 2 orders of magnitude larger than the resistivity of the Pt layer suggests that if there was no thermally induced spin pumping from the FM to the PM, the anomalous Nernst voltage on the Fe_3O_4 layer would be strongly suppressed by the Pt top layer. Therefore, the voltage signal in the Pt/Fe_3O_4 sample must be dominated by the SSE. To estimate the suppression of the ANE signal upon placement of the Pt layer, we consider the expression from the electron transport theory $J_m^i = \sigma_m^{ij} E^j - \alpha_m^{ik} \nabla_k T$, where J_m^i stands for the electron current, E^j is the electric field, $\nabla_k T$ is the applied thermal gradient, and the coefficients σ_m^{ij} and α_m^{ik} are the elements of the conductivity and thermopower tensor, respectively. Under our experimental conditions, we obtain the following expressions:

$$\begin{aligned} J_I^z &= \sigma_I^{zz} E^z + \sigma_I^{zy} E^y - \alpha_I^{zz} (\nabla_z T)_I, \\ J_I^y &= \sigma_I^{yz} E^z + \sigma_I^{yy} E^y - \alpha_I^{zy} (\nabla_z T)_I, \\ J_{II}^z &= \sigma_{II}^{zz} E^z - \alpha_{II}^{zz} (\nabla_z T)_{II}, \\ J_{II}^y &= \sigma_{II}^{yy} E^y, \end{aligned} \tag{3}$$

where $m = I$ and $m = II$ describe the FM (in the experiment, Fe_3O_4) and PM (in the experiment, Pt), respectively. Note that, in the transport equation above, the cross relation between charge and spin current is neglected, this assumption is supported by recent experiments by Kikkawa *et al.*[32] Considering the open circuit condition: $I^z = A_0 J_I^z = A_0 J_{II}^z = 0$ and $I^y = S_I J_I^y + S_{II} J_{II}^y = 0$, with $A_0 = L_x L_y$ and $S_m = L_x t_m$ being the area of the film with normal to the z and y direction, respectively. The following expression for the transversal component E^y is obtained:

$$E^y = \left(\frac{r}{1+r} \right) E_{ANE}, \tag{4}$$

where $r = \frac{\rho_{Pt}}{\rho_{Fe_3O_4}} \frac{t_{Fe_3O_4}}{t_{Pt}}$ and $E_{ANE} = [\frac{\alpha^{yz}}{\sigma^{zz}} - (\frac{\sigma^{yz}}{\sigma^{zz}} \frac{\alpha^{zz}}{\sigma^{zz}})](\nabla_z T)_{Fe_3O_4}$ is the anomalous Nernst signal measured in the Fe_3O_4 film. Considering a resistivity value of 4.8×10^{-7} Ωm for a Pt film grown under similar conditions[33] and 5×10^{-5} Ωm for the

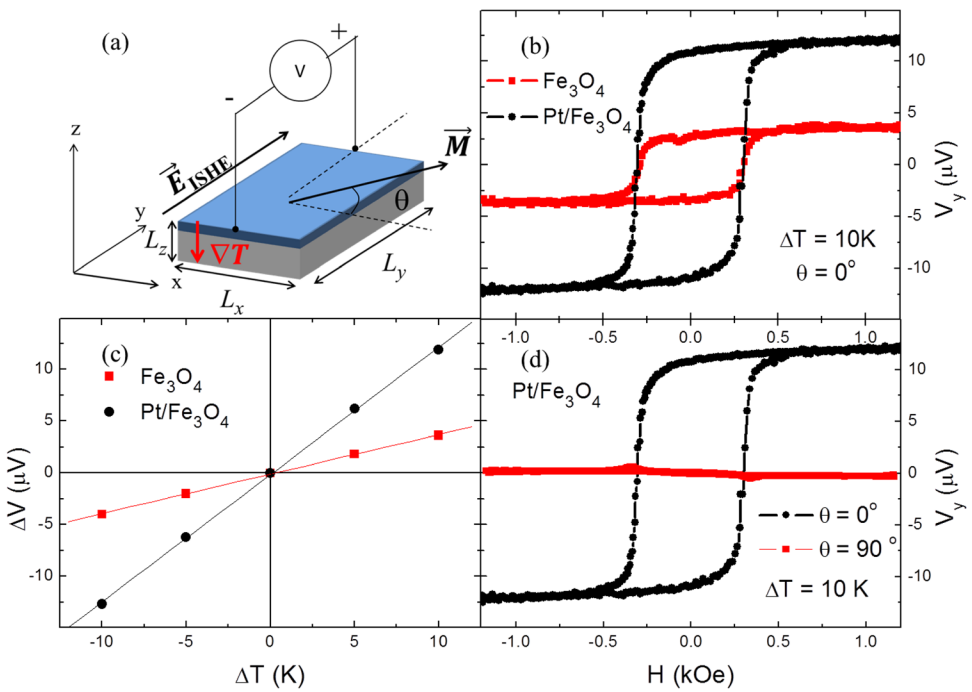

FIG. 1. (a) Schematic illustration of the measurement setup. (b) Obtained results for the Fe_3O_4 film with and without the Pt detecting layer at room temperature. (c) Dependence of ΔV measured at different magnitudes of the temperature difference (ΔT) across the sample with and without Pt layer at room temperature. (d) Angular dependence of the measured voltage (V_y) in the Pt/Fe_3O_4 system at room temperature.

This article is copyrighted as indicated in the article. Reuse of AIP content is subject to the terms at: http://scitation.aip.org/termsconditions. Downloaded to IP: 161.111.180.191 On: Wed, 08 Jul 2015 09:55:11

50 nm Fe_3O_4 film, we obtain that the ANE signal in the Pt/Fe_3O_4 sample is reduced to 10% of the ANE signal in the Fe_3O_4 sample, giving a contribution of about 3% to the total observed signal $V_y = E^y L_y$ in Pt/Fe_3O_4. This is a strong indication that the spin Seebeck effect is the dominant contribution to the observed voltage. Measurements at different magnitudes of the thermal gradient with the magnetic field applied in the x direction were also performed. Figure 1(c) shows the linear dependence of $\Delta V = (V_y(+H) - V_y(-H))/2$ with ΔT, as it is expected. From the slope of these curves, we can extract the coefficients for the SSE and ANE, for the Pt/Fe_3O_4 and Fe_3O_4 sample, respectively. In order to evaluate the magnitude of the spin Seebeck effect, we define the coefficient $S_{zy} = (\Delta V/\Delta T)(L_z/L_y)$, where L_z is the length of the sample in the direction of the applied temperature gradient (see Fig. 1(a)). This coefficient is independent of the sample size and enables quantitative comparison between experiments with different geometries.[32] Considering the correction for the shorting effect of the ANE in Fe_3O_4 due to the Pt layer, described above, we obtain a value of the SSE at room temperature of $S_{zy} = 74 \pm 1$ nV/K. Measurements on the dependence of the direction of the applied magnetic field were also performed (see Fig. 1(d)), and it can be observed that when the field is parallel to the direction in which the voltage is measured $\theta = 90°$, the voltage vanishes, in agreement with Eq. (1).

The longitudinal SSE configuration is normally used for insulating samples; therefore, it is interesting to measure the effect at temperatures below the Verwey transition ($T_V = 115$ K), after the sample undergoes the metal to insulator transition. Figure 2 shows that the ANE in Fe_3O_4 could not be detected below $T = 110$ K, due to the very high electrical resistance as a consequence of the strong reduction of charge carriers in the insulating phase. The reduction of the ANE below T_V is in a stark contrast to the behavior of the thermopower which does not become immeasurable below the Verwey transition,[34] the physics behind the measured ANE reported here is yet to be understood. The temperature dependence of the ANE above the transition temperature resembles that of the thermal conductivity of the substrate,[35] this will be the subject of subsequent studies. Here, we will focus on the observation of the SSE below the Verwey transition. It is interesting to point out that despite the suppression of the ANE, the SSE can still be detected for $T < T_V$, as it is shown in Fig. 3(a) for $T = 105$ K. This is a strong indication of the observation of pure spin Seebeck effect. We estimated a SSE coefficient (S_{zy}) at this temperature of about 52 ± 12 nV/K. It can be observed that there is a reduction of the SSE compared to the value observed at 300 K, this could be possibly related to the changes induced by the Verwey transition on the thermal[36,37] and magnetic[38,39] properties of the film, which can affect the thermal spin pumping at the Fe_3O_4/Pt interface and therefore the observed SSE signal.

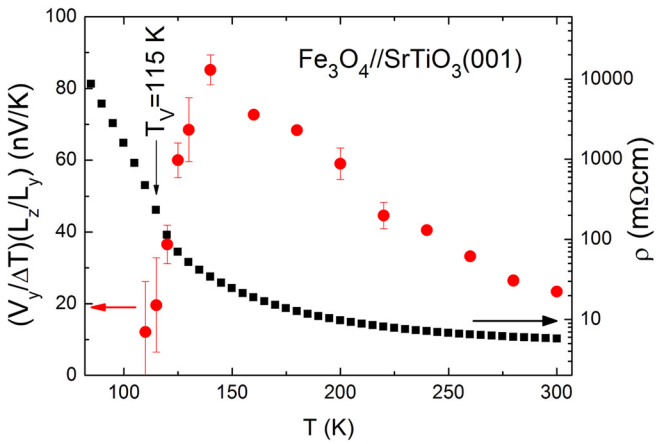

FIG. 2. Temperature dependence of the electrical resistivity (squares) and the geometrically corrected anomalous Nernst voltage normalized with the applied temperature difference (circles) for the Fe_3O_4(001)//$SrTiO_3$(001) sample.

We proceed to estimate the contribution of the ANE due to magnetic proximity[40] in the Pt layer. In order to do so, we consider the Pt layer to be divided into a magnetic and a non-magnetic region with thicknesses d_I and d_{II}, respectively (see Fig. 3(b)). From the electron transport equations $J^i = \sigma^{ij}E^j - \alpha^{ij}\nabla_j T$, we obtain a similar expression to that observed in Eq. (3), with I and II correspondent to the magnetic and non-magnetic regions of the Pt layer, respectively. Considering the open circuit condition as described previously, we obtain the following expression for the transversal electric field:

$$E^y = \left(\frac{d_I}{d_I + d_{II}}\right) E^*_{ANE}, \tag{5}$$

where the parameter $\frac{d_I}{d_I+d_{II}}$ accounts for the shorting of the ANE of the magnetized region by the non-magnetized region within the Pt layer and $E^*_{ANE} = \left\{\frac{\alpha^{yz}}{\sigma^{zz}} - \frac{\sigma^{yz}}{\sigma^{zz}}\frac{\alpha^{zz}}{\sigma^{zz}}\right\}(\nabla T)_{Pt} = V^{MP}_{ANE}/L_y$ is the

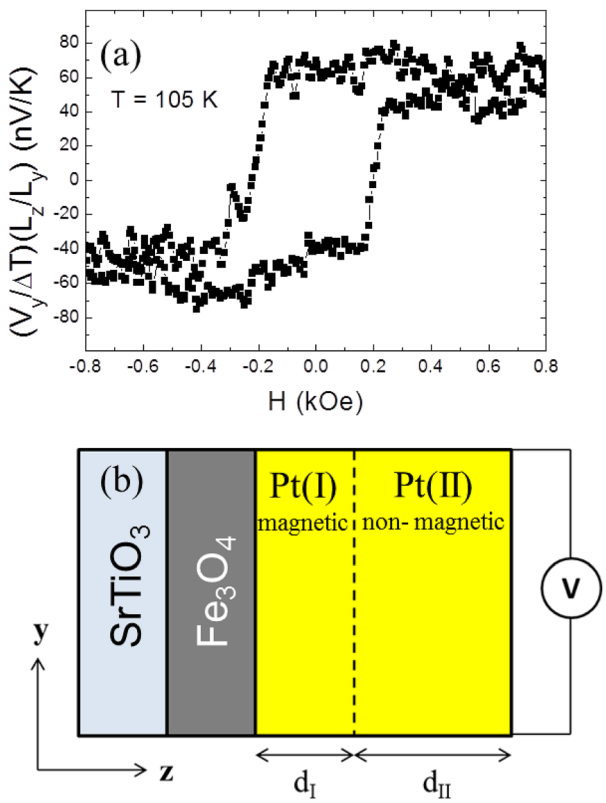

FIG. 3. (a) Magnetic field dependence of the spin Seebeck effect measured at 105 K. (b) Schematic used to estimate the ANE due to magnetic proximity in the Pt layer.

This article is copyrighted as indicated in the article. Reuse of AIP content is subject to the terms at: http://scitation.aip.org/termsconditions. Downloaded to IP: 161.111.180.191 On: Wed, 08 Jul 2015 09:55:11

ANE of the magnetized Pt region. To estimate this quantity, we use the coefficients for the conductivity and thermopower tensor previously measured in FePt thin films.[41] An estimation of the thermal gradient across the Pt thin film can be obtained by considering that the heat is conserved across the different interfaces of our system. For $t_{STO} \gg t_{Fe_3O_4}, t_{Pt}$ and using the tabulated values for thermal conductivity of $SrTiO_3$ and Pt,[42] we obtained $(\nabla T)_{Pt} \approx 3.75 \times 10^2 \Delta T$ in K/m, with ΔT being the temperature difference generated between the hot and cold sides of our sample. We obtained an expression for the upper limit of the contribution due to magnetic proximity in the Pt layer to the observed effect

$$\frac{V_{ANE}^{MP}}{\Delta T}\frac{L_z}{L_y} \leq 7.5n\,[\mathrm{nV/K}], \tag{6}$$

where n is the number of monolayers of Pt which are fully magnetized. If we consider one monolayer of Pt to be fully magnetized $(n=1)$,[43] we obtain a contribution due to the proximity effect of 7.5 nV/K. This value is almost one order of magnitude smaller than the effect observed at 105 K and comparable to the error of the measurement; therefore, the thermally induced voltage is clearly dominated by the SSE.

In conclusion, we have observed the spin Seebeck effect in magnetite film. At room temperature, despite of the fact that the films are electrically conductive, the contribution of the ANE effect of magnetite only accounts for 3% of the observed signal, due to the resistivity difference between Fe_3O_4 and Pt films. The ANE signal falls under the detection values below the Verwey transition, this points to a suppression of the ANE as a consequence of the reduction of charge carriers. Therefore at temperatures below T_V, the SSE signal is free from any contamination from ANE of the ferromagnetic layer. The effect of the magnetic proximity in Pt has also been evaluated below the metal-insulator transition and it has been observed to be one order of magnitude smaller than the measured signal, clearly showing that the SSE is the dominant contribution in our measurements.

R. Ramos and T. Kikkawa contributed equally on the thermal transport measurements. This work was supported by the Spanish Ministry of Science (through projects PLE2009-0017, PRI-PIBJP-2011-0794, MAT2011-27553-C02, including FEDER funding) and the Aragón Regional Government (project E26). This research was supported by Strategic International Cooperative Program, Japan Science and Technology Agency (JST), PRESTO-JST "Phase Interfaces for Highly Efficient Energy Utilization," CREST-JST "Creation of Nanosystems with Novel Functions through Process Integration," a Grant-in-Aid for Research Activity Start-up (24860003) from MEXT, Japan, a Grant-in-Aid for Scientific Research (A) (24244051) from MEXT, Japan, LC-IMR of Tohoku University, the Murata Science Foundation, and the Mazda Foundation.

[1]J. P. Heremans, V. Jovovic, E. S. Toberer, A. Saramat, K. Kurosaki, A. Charoenphakdee, S. Yamanaka, and G. J. Snyder, Science **321**, 554 (2008).
[2]H. Jin, C. M. Jaworski, and J. P. Heremans, Appl. Phys. Lett. **101**, 053904 (2012).
[3]G. E. W. Bauer, E. Saitoh, and B. J. van Wees, Nature Mater. **11**, 391 (2012).
[4]G. E. W. Bauer, A. H. MacDonald, and S. Maekawa, Solid State Commun. **150**, 459 (2010).
[5]B. Scharf, A. Matos-Abiague, I. Žutić, and J. Fabian, Phys. Rev. B **85**, 085208 (2012).
[6]M. Hatami, G. E. W. Bauer, Q. Zhang, and P. J. Kelly, Phys. Rev. B **79**, 174426 (2009).
[7]J.-C. Le Breton, S. Sharma, H. Saito, S. Yuasa, and R. Jansen, Nature **475**, 82 (2011).
[8]H. Yu, S. Granville, D. P. Yu, and J.-P. Ansermet, Phys. Rev. Lett. **104**, 146601 (2010).
[9]M. V. Costache, G. Bridoux, I. Neumann, and S. O. Valenzuela, Nature Mater. **11**, 199 (2012).
[10]K. Uchida, S. Takahashi, K. Harii, J. Ieda, W. Koshibae, K. Ando, S. Maekawa, and E. Saitoh, Nature **455**, 778 (2008).
[11]A. Slachter, F. L. Bakker, J.-P. Adam, and B. J. van Wees, Nat. Phys. **6**, 879 (2010).
[12]J. Flipse, F. L. Bakker, A. Slachter, F. K. Dejene, and B. J. van Wees, Nat. Nanotechnol. **7**, 166 (2012).
[13]E. Saitoh, M. Ueda, H. Miyajima, and G. Tatara, Appl. Phys. Lett. **88**, 182509 (2006).
[14]K. Uchida, T. Ota, K. Harii, K. Ando, H. Nakayama, and E. Saitoh, J. Appl. Phys. **107**, 09A951 (2010).
[15]C. M. Jaworski, J. Yang, S. Mack, D. D. Awschalom, J. P. Heremans, and R. C. Myers, Nature Mater. **9**, 898 (2010).
[16]C. M. Jaworski, J. Yang, S. Mack, D. D. Awschalom, R. C. Myers, and J. P. Heremans, Phys. Rev. Lett. **106**, 186601 (2011).
[17]C. M. Jaworski, R. C. Myers, E. Johnston-Halperin, and J. P. Heremans, Nature **487**, 210 (2012).
[18]K. Uchida, J. Xiao, H. Adachi, J. Ohe, S. Takahashi, J. Ieda, T. Ota, Y. Kajiwara, H. Umezawa, H. Kawai *et al.*, Nature Mater. **9**, 894 (2010).
[19]K. Uchida, T. Nonaka, T. Yoshino, T. Kikkawa, D. Kikuchi, and E. Saitoh, Appl. Phys. Express **5**, 093001 (2012).
[20]H. Adachi, J.-i. Ohe, S. Takahashi, and S. Maekawa, Phys. Rev. B **83**, 094410 (2011).
[21]H. Adachi, K. Uchida, E. Saitoh, and S. Maekawa, Rep. Prog. Phys. **76**, 036501 (2013).
[22]J. Xiao, G. E. W. Bauer, K. Uchida, E. Saitoh, and S. Maekawa, Phys. Rev. B **81**, 214418 (2010).
[23]J. Sinova and I. Zutic, Nature Mater. **11**, 368 (2012).
[24]R. Ramos, S. K. Arora, and I. V. Shvets, Phys. Rev. B **78**, 214402 (2008).
[25]K. Balakrishnan, S. K. Arora, and I. V. Shvets, J. Phys.: Condens. Matter. **16**, 5387 (2004).
[26]H.-C. Wu, M. Abid, B. S. Chun, R. Ramos, O. N. Mryasov, and I. V. Shvets, Nano Lett. **10**, 1132 (2010).
[27]A. Fernandez-Pacheco, J. Orna, J. M. D. Teresa, P. A. Algarabel, L. Morellón, J. A. Pardo, M. R. Ibarra, E. Kampert, and U. Zeitler, Appl. Phys. Lett. **95**, 262108 (2009).
[28]F. Walz, J. Phys.: Condens. Matter. **14**, R285 (2002).
[29]J. Orna, P. A. Algarabel, L. Morellón, J. A. Pardo, J. M. de Teresa, R. López Antón, F. Bartolomé, L. M. García, J. Bartolomé, J. C. Cezar *et al.*, Phys. Rev. B **81**, 144420 (2010).
[30]K. Uchida, T. Ota, H. Adachi, J. Xiao, T. Nonaka, Y. Kajiwara, G. E. W. Bauer, S. Maekawa, and E. Saitoh, J. Appl. Phys. **111**, 103903 (2012).
[31]M. Weiler, M. Althammer, F. D. Czeschka, H. Huebl, M. S. Wagner, M. Opel, I.-M. Imort, G. Reiss, A. Thomas, R. Gross *et al.*, Phys. Rev. Lett. **108**, 106602 (2012).
[32]T. Kikkawa, K. Uchida, Y. Shiomi, Z. Qiu, D. Hou, D. Tian, H. Nakayama, X.-F. Jin, and E. Saitoh, Phys. Rev. Lett. **110**, 067207 (2013).
[33]A. Kirihara, K. Uchida, Y. Kajiwara, M. Ishida, Y. Nakamura, T. Manako, E. Saitoh, and S. Yorozu, Nature Mater. **11**, 686 (2012).
[34]D. Kim and J. M. Honig, Phys. Rev. B **49**, 4438 (1994).
[35]C. Yu, M. L. Scullin, M. Huijben, R. Ramesh, and A. Majumdar, Appl. Phys. Lett. **92**, 191911 (2008).
[36]A. Salazar, A. Oleaga, A. Wiechec, Z. Tarnawski, and A. Kozlowski, IEEE Trans. Magn. **40**, 2820 (2004).
[37]G. A. Slack, Phys. Rev. **126**, 427 (1962).
[38]R. Reznícek, V. Chlan, H. Stěpánková, P. Novák, and M. Marysko, J. Phys.: Condens. Matter **24**, 055501 (2012).
[39]R. J. McQueeney, M. Yethiraj, W. Montfrooij, J. S. Gardner, P. Metcalf, and J. M. Honig, Phys. Rev. B **73**, 174409 (2006).
[40]S. Y. Huang, X. Fan, D. Qu, Y. P. Chen, W. G. Wang, J. Wu, T. Y. Chen, J. Q. Xiao, and C. L. Chien, Phys. Rev. Lett. **109**, 107204 (2012).

This article is copyrighted as indicated in the article. Reuse of AIP content is subject to the terms at: http://scitation.aip.org/termsconditions. Downloaded to IP: 161.111.180.191 On: Wed, 08 Jul 2015 09:55:11

[41]M. Mizuguchi, S. Ohata, K. Uchida, E. Saitoh, and K. Takanashi, Appl. Phys. Express **5**, 093002 (2012).
[42]D. Lide, *CRC Handbook of Chemistry & Physics* (Taylor & Francis Group, 2009).
[43]F. Wilhelm, P. Poulopoulos, G. Ceballos, H. Wende, K. Baberschke, P. Srivastava, D. Benea, H. Ebert, M. Angelakeris, N. K. Flevaris *et al.*, Phys. Rev. Lett. **85**, 413 (2000). The authors report layer resolved magnetic moment studies on Ni/Pt multilayers. These experiments show that the Pt has a magnetic moment at the interface with Ni, although it is not fully magnetized. Therefore, we have considered an upper limit of one monolayer of Pt to be fully magnetized (n = 1) for our estimation.

This article is copyrighted as indicated in the article. Reuse of AIP content is subject to the terms at: http://scitation.aip.org/termsconditions. Downloaded to IP: 161.111.180.191 On: Wed, 08 Jul 2015 09:55:11